



Phase Behavior of Selected Condensed Double-Decker Shaped Silsesquioxane Compounds

David F. Vogelsang¹ · Robert E. Maleczka Jr² · Andre Lee¹

Received: 16 July 2021 / Accepted: 11 October 2021

© Springer Nature B.V. 2021

Abstract

Bisfunctional dichlorosilanes were reacted with tetrasilanol of double-decker shaped octaphenylsilsesquioxane (DDSQ) to form fully condensed DDSQ compounds. The crystallographic and thermal characteristics of these compounds were examined. For compounds capped with dichlorosilanes bearing linear aliphatic moieties, as the number of carbon increases from methyl to *n*-butyl (from 1 to 4) the melting temperature, T_m , dropped from 546 K to 416 K. While for compounds capped with cycloaliphatic, as the moiety changes from cyclopentyl to cyclohexyl, the value of T_m increases from 533 K to 555 K. Surprising, the highest T_m observed was that when capping was done using diisopropyl dichlorosilane. A T_m of around 565 K was observed, which was even higher as compare to diphenyl dichlorosilane capped DDSQ, which had T_m of about 526 K. Phase behavior of binary and ternary mixtures of these condensed DDSQ was also investigated. To our surprise, mixtures of these compounds form eutectic. The eutectic points were calculated based on ideal binary and ternary eutectic from the thermal properties of pure components. Depending on the crystallography, experimental observations of eutectic match well with calculated values.

Keywords Double-decker shaped silsesquioxanes · Eutectic · Ternary · Binary · Mixtures

1 Introduction

Reacting tetrasilanol of double-decker shaped octaphenyl silsesquioxane $\text{DDSQ}(\text{OH})_4$ with an appropriate quantity of dichlorosilanes ($\text{RR}'\text{SiCl}_2$) or difluorosilanes ($\text{RR}'\text{SiF}_2$) can result in a fully condensed structure ($\text{DDSQ-2}(\text{RR}')$) as observed in Scheme 1 [1–9]. These compounds have been used to form hybrid polymers with silsesquioxane as a part of the backbone [3, 6, 10]. To the date few reviews has been developed over double decker silsesquioxane chemistry and properties. Mainly because to these structures are relative recent in the literature [11, 12]. These hybrid polymers exhibit lower contact angles, lower dielectric constant, and higher

flammability resistance, with a minimal impact on the mechanical and optical properties with respect to control polymers [6, 13–19]. It was recognized for R different than R', the as-synthesized product is a mixture of *cis* and *trans* isomers about the double-decker shaped silsesquioxane core [1, 2, 4, 5, 20–22]. Isolation of these isomers can be achieved by selective solvent fractional crystallization, liquid chromatography, or a combination of both depending on the chemical moiety of R and R' [2, 5, 9, 20–22].

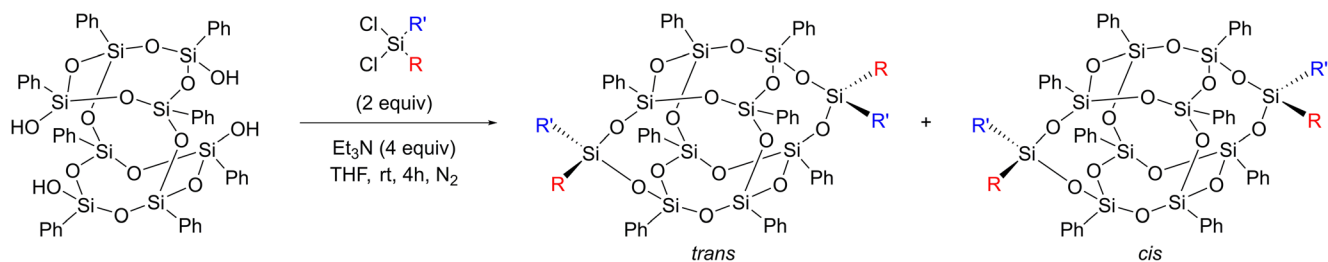
Once separated, it was demonstrated that *cis* $\text{DDSQ-2}(\text{RR}')$ has a different crystallographic structure than *trans* $\text{DDSQ-2}(\text{RR}')$ as well as different thermal and physical properties [4, 5, 9, 10, 21]. Recently, the phase behavior of *cis* and *trans* $\text{DDSQ-2}(\text{RR}')$ binary mixtures where R was methyl and R' was phenyl, aniline, or 1,4-phenylethynyl(phenyl) was reported [21]. From the study, it was determined that the bulkier moiety has a reductive effect on the melting temperature of isolated *cis* and *trans* isomers. Due to the complete miscibility in the liquid-state and immiscibility in the solid-state, it was possible to obtain a eutectic *cis-trans* composition. Mixtures with a eutectic composition are important in many industries including pharmaceutical, thermosetting resins formulation, or metallic alloys as lower solid-to-liquid temperature enables better processability [23–27].

✉ Robert E. Maleczka, Jr
maleczka@chemistry.msu.edu

✉ Andre Lee
leea@egr.msu.edu

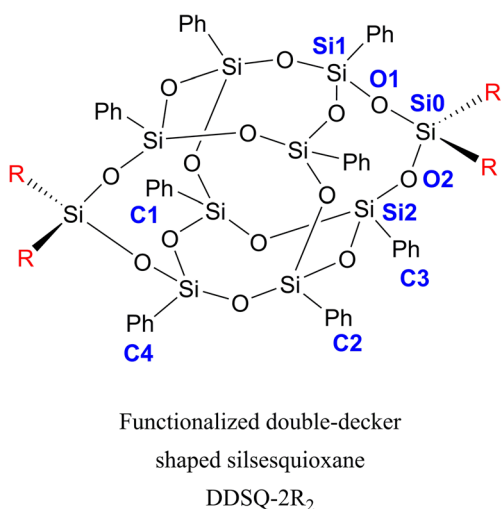
¹ Department of Chemical Engineering and Materials Science, Michigan State University, 428 S. Shaw Lane, Room 2100, East Lansing, MI 48824-1226, USA

² Department of Chemistry, Michigan State University, 578 S. Shaw Lane, East Lansing, MI 48824-1322, USA



Scheme 1 Functionalization of DDSQ-OH₄ with dichlorosilanes

It would be interesting to further explore the possible processing advantages and to have a deeper understanding of the cause of the immiscibility in the solid-state of different completely condensed DDSQ compounds. However, the progress of such explorations can be limited by the need to perform separation after the synthesis, as well as the relative difficulties in achieving high isomeric purity for DDSQ-2(RR'). In this work, seven different bis-functional dichlorosilanes (R₂SiCl₂) were used in the capping reaction to form fully condensed DDSQ-2R₂, as seen in Scheme 2. In this approach, the complexity of geometric isomer formation is eliminated, and the purity of the desired compound can be assured with simple column chromatography after the synthesis. Hence, the effect of the R group bonded to the D-silicon (the siloxane) group on the crystal structure, as well as the melting and recrystallization behavior of completely condensed DDSQ compounds, can be more effectively investigated as a single compound. It was decided to evaluate if systems with different functional groups could also have partial miscibility in the solid-state. To achieve this goal, binary and ternary mixtures from the seven synthesized structures were mixed, and their solid-liquid phase behavior evaluated.



Scheme 2 DDSQ-2R₂ structure and R groups used for this work are methyl (Me); ethyl (Et); isopropyl (*i*Pr); *n*-butyl (*n*Bu); cyclopentyl (CyP); cyclohexyl (CyH); phenyl (Ph).

2 Experimental

2.1 Materials

All materials were used as received unless otherwise indicated. (C₆H₅)₈Si₈O₁₀(OH)₄ 5,11,14,17-Tetra(hydro)octaphenyltetracyclo[7.3.3.-3^{3,7}]octasilsesquioxane or DDSQ-(Ph)₈(OH)₄ was obtained from Hybrid Plastics, Inc. (CH₃)₂SiCl₂ di-methyl dichlorosilane, (C₂H₅)₂SiCl₂ di-ethyl dichlorosilane, (CHC₂H₆)₂SiCl₂ di-isopropyl dichlorosilane, (C₄H₉)₂SiCl₂ di-*n*-butyl dichlorosilane, (C₅H₉)₂SiCl₂ di-cyclopentyl dichlorosilane, (C₆H₁₁)₂SiCl₂ dicyclohexyl dichlorosilane, and (C₆H₅)₂SiCl₂ di-phenyl dichlorosilane were purchased from Gelest. Triethylamine (Et₃N) was purchased from Avantor. Tetrahydrofuran (THF) obtained from Fisher was refluxed over sodium/ benzophenone ketyl and distilled. Deuterated chloroform with 1 vol.% of tetramethylsilane CDCl₃-TMS was obtained from Sigma.

3 Methods

3.1 General Synthetic Procedure

A 500 mL round bottom flask equipped with a magnetic stirrer was flushed with a N₂ stream for 15 min. Afterwards, 4.00 g (3.74 mmol) of DDSQ-(Ph)₈(OH)₄ (1) were added followed by 200 mL of THF. The flask was then sealed with a rubber septum and attached to a dry N₂ hose from a Schlenk line. (R₂)SiCl₂ (7.85 mmol) was added by syringe through the rubber septum. Then, 2.19 mL (15.71 mmol) of Et₃N were added dropwise over 5 min forming a cloudy suspension. The reactions were run for 12 h and then the triethylamine hydrochloride salt was filtered off from the solution using a fritter funnel filter. The volatiles in the clear filtrate were evaporated under dynamic vacuum for 30 min to afford a white powder. This powder was then solubilized in DCM and crystallized by addition of hexanes or methanol to remove possible impurities in the samples.

3.2 Synthesis of (C₆H₅)₈Si₁₀O₁₄(CH₃)₄ 7,7,17,17-Tetramethyl-1,3,5,9,11,13,15,1-Octaphenylhexacyclo[9.13.1^{1,9}.1^{3,15}.1^{5,13}.1^{11,19}] Decasiloxane - DDSQ-2Me₂ (2)

Compound **2** was synthesized using the general procedure with (CH₃)₂SiCl₂ (7.85 mmol, 0.96 mL). This provided 4.01 g (91% yield) of compound **2** as a white powder. ¹H NMR (500 MHz, CDCl₃): δ ppm 0.33 (s, 12H), 7.22 (t, *J* = 7.3 Hz, 8H), 7.28 (t, *J* = 7.1 Hz, 8H), 7.37 (tt, *J*₁ = 7.3 Hz, *J*₂ = 1.4 Hz, 4H), 7.43 (tt, *J*₁ = 7.3 Hz, *J*₂ = 1.4 Hz, 4H), 7.46 (dd, *J*₁ = 6.8 Hz, *J*₂ = 1.3 Hz, 8H), 7.54 (dd, *J*₁ = 7.8 Hz, *J*₂ = 1.5 Hz, 8H) ¹³C NMR (126 MHz, CDCl₃): δ ppm 0.58, 127.79, 130.39, 131.25, 132.30, 134.13 ²⁹Si NMR (99 MHz, CDCl₃): δ ppm -16.61 (s, 2Si), -78.62 (s, 4Si), -79.59 (s, 4Si).

3.3 Synthesis of (C₆H₅)₈Si₁₀O₁₄(C₂H₅)₄ 7,7,17,17-Tetraethyl-1,3,5,9,11,13,15,1-Octaphenylhexacyclo[9.13.1^{1,9}.1^{3,15}.1^{5,13}.1^{11,19}] Decasiloxane - DDSQ-2Et₂ (3)

Compound **3** was synthesized using the general procedure with (C₂H₅)₂SiCl₂ (7.85 mmol, 1.18 mL). This provided 3.13 g (68% yield) of compound **3** as a white powder. ¹H NMR (500 MHz, CDCl₃): δ ppm 0.73 (q, *J* = 7.8 Hz, 8H), 1.02 (t, *J* = 8 Hz, 12H), 7.21 (t, *J* = 7.6 Hz, 8H), 7.27 (t, *J* = 7.5 Hz, 8H), 7.36 (tt, *J*₁ = 7.4 Hz, *J*₂ = 1.2 Hz, 4H), 7.41 (tt, *J*₁ = 7.4 Hz, *J*₂ = 1.4 Hz, 4H), 7.45 (dd, *J*₁ = 6.8 Hz, *J*₂ = 1.1 Hz, 8H), 7.54 (dd, *J*₁ = 8.1 Hz, *J*₂ = 1.2 Hz, 8H) ¹³C NMR (126 MHz, CDCl₃): δ ppm 6.33, 6.91, 127.66, 130.23, 131.16, 132.21, 133.96 ²⁹Si NMR (99 MHz, CDCl₃): δ ppm -79.74 (s, 4Si), -78.92 (s, 4Si), -16.96 (s, 2Si).

3.4 Synthesis of (C₆H₅)₈Si₁₀O₁₄(CH(CH₃)₂)₄ 7,7,17,17-Tetra-isopropyl-1,3,5,9,11,13,15,1-Octaphenylhexacyclo[9.13.1^{1,9}.1^{3,15}.1^{5,13}.1^{11,19}] Decasiloxane - DDSQ-2iPr₂ (4)

Compound **4** was synthesized using the general procedure with (CH(CH₃)₂)₂SiCl₂ (7.85 mmol, 1.42 mL). This provided 3.59 g (74% yield) of compound **4** as a white powder. ¹H NMR (500 MHz, CDCl₃): δ ppm 1.05 (s, 24H), 1.27 (s, 4H), 7.19 (t, *J* = 7.6 Hz, 8H), 7.24 (t, *J* = 7.5 Hz, 8H), 7.34 (tt, *J*₁ = 7.6 Hz, *J*₂ = 1.3 Hz, 4H), 7.38 (tt, *J*₁ = 7.6 Hz, *J*₂ = 1.4 Hz, 4H), 7.43 (dd, *J*₁ = 7.8 Hz, *J*₂ = 1.4 Hz, 8H), 7.55 (dd, *J*₁ = 7.8 Hz, *J*₂ = 1.3 Hz, 8H) ¹³C NMR (126 MHz, CDCl₃): δ ppm 12.87, 16.77, 127.68, 130.22, 131.20, 132.25, 133.98 ²⁹Si NMR (99 MHz, CDCl₃): δ ppm -79.82 (s, 4Si), -79.40 (s, 4Si), -19.69 (s, 2Si).

3.5 Synthesis of (C₆H₅)₈Si₁₀O₁₄(C₄H₉)₄ 7,7,17,17-Tetra-*n*-Butyl-1,3,5,9,11,13,15,1-Octaphenylhexacyclo[9.13.1^{1,9}.1^{3,15}.1^{5,13}.1^{11,19}] Decasiloxane - DDSQ-2*n*Bu₂ (5)

Compound **5** was synthesized using the general procedure with (C₄H₉)₂SiCl₂ (7.85 mmol, 1.69 mL). This provided 3.78 g (75% yield) of compound **5** as a white powder. ¹H NMR (500 MHz, CDCl₃): δ ppm 0.72–0.74 (overlaped, 20H), 1.28 (sxt, *J* = 7.3 Hz, 8H), 1.43 (m, 8H), 7.18 (t, *J* = 7.7 Hz, 8H), 7.26 (t, *J* = 7.7 Hz, 8H), 7.34 (tt, *J*₁ = 7.4 Hz, *J*₂ = 1.1 Hz, 4H), 7.40 (tt, *J*₁ = 7.6 Hz, *J*₂ = 1.4 Hz, 4H), 7.44 (dd, *J*₁ = 7.8 Hz, *J*₂ = 1.3 Hz, 8H), 7.56 (dd, *J*₁ = 8.1 Hz, *J*₂ = 1.2 Hz, 8H) ¹³C NMR (126 MHz, CDCl₃): δ ppm 13.66, 15.46, 24.85, 26.12, 127.63, 130.23, 131.16, 132.29, 134.01 ²⁹Si NMR (99 MHz, CDCl₃): δ ppm -79.73 (s, 4Si), -78.99 (s, 4Si), -18.43 (s, 2Si).

3.6 Synthesis of (C₆H₅)₈Si₁₀O₁₄(C₆H₁₁)₄ 7,7,17,17-Tetracyclopentyl-1,3,5,9,11,13,15,1-Octaphenylhexacyclo[9.13.1^{1,9}.1^{3,15}.1^{5,13}.1^{11,19}] Decasiloxane - DDSQ-2CyP₂ (6)

Compound **6** was synthesized using the general procedure with (C₅H₉)₂SiCl₂ (7.85 mmol, 1.68 mL). This provided 3.59 g (69% yield) of compound **6** as a white powder. ¹H NMR (500 MHz, CDCl₃): δ ppm 1.11 (m, 4H), 1.45 (m, 8H), 1.57 (m, 16H), 1.78 (m, 8H), 7.19 (t, *J* = 7.6 Hz, 8H), 7.25 (t, *J* = 7.6 Hz, 8H), 7.34 (tt, *J*₁ = 7.6 Hz, *J*₂ = 1.2 Hz, 4H), 7.39 (t, *J*₁ = 7.6 Hz, *J*₂ = 1.2 Hz, 4H), 7.43 (dd, *J*₁ = 7.8 Hz, *J*₂ = 1.3 Hz, 8H), 7.54 (dd, *J*₁ = 7.8 Hz, *J*₂ = 1.4 Hz, 8H). ¹³C NMR (126 MHz, CDCl₃): δ ppm 24.95, 26.98, 27.20, 127.52, 130.15, 131.24, 132.38, 133.94 ²⁹Si NMR (99 MHz, CDCl₃): δ ppm -79.79 (s, 4Si), -79.37 (s, 4Si), -20.43 (s, 2Si).

3.7 Synthesis of (C₆H₅)₈Si₁₀O₁₄(C₆H₅)₄ 7,7,17,17-Tetracyclohexyl-1,3,5,9,11,13,15,1-Octaphenylhexacyclo[9.13.1^{1,9}.1^{3,15}.1^{5,13}.1^{11,19}] Decasiloxane - DDSQ-2CyH₂ (7)

Compound **7** was synthesized using the general procedure with (C₆H₁₁)₂SiCl₂ (7.85 mmol, 1.89 mL). This provided 3.44 g (63% yield) of compound **7** as a white powder. ¹H NMR (500 MHz, CDCl₃): δ ppm 0.86 (tt, *J*₁ = 12.5 Hz, *J*₂ = 3.1 Hz, 4H), 1.14 (bs, 12H), 1.3 (q, *J* = 12.4 Hz, 8H), 1.63 (d, *J*₁ = 6.4 Hz, 12H), 1.80 (d, *J*₁ = 13.2 Hz, 8H), 7.18 (t, *J* = 7.7 Hz, 8H), 7.26 (t, *J* = 7.7 Hz, 8H), 7.34 (tt, *J*₁ = 7.6 Hz, *J*₂ = 1.2 Hz, 4H), 7.40 (tt, *J*₁ = 7.6 Hz, *J*₂ = 1.4 Hz, 4H), 7.43 (dd, *J*₁ = 7.8 Hz, *J*₂ = 1.1 Hz, 8H), 7.56 (dd, *J*₁ = 7.8 Hz, *J*₂ = 1.1 Hz, 8H) ¹³C NMR (126 MHz, CDCl₃): δ ppm 24.75, 26.51, 26.79, 27.60, 127.61, 130.17, 131.21, 132.34, 133.99

^{29}Si NMR (99 MHz, CDCl_3): δ ppm -79.74 (s, 4Si), -79.41 (s, 4Si), -24.03 (s, 2Si).

3.8 Synthesis of $(\text{C}_6\text{H}_5)_8\text{Si}_{10}\text{O}_{14}(\text{C}_6\text{H}_5)_4$ 7,7,17,17-Tetraphenyl-1,3,5,9,11,13,15,1-Octaphenylhexacyclo[9.13.1^{1,9}.1^{3,15}.1^{5,13}.1^{11,19}]Decasiloxane - DDSQ-2Ph₂ (8)

Compound **8** was synthesized using the general procedure with $(\text{C}_6\text{H}_5)_2\text{SiCl}_2$ (7.85 mmol, 1.65 mL). This provided 3.78 g (71% yield) of compound **8** as a white powder. ^1H NMR (500 MHz, CDCl_3): δ ppm 7.1 (t, $J = 7.6$ Hz, 8H), 7.17 (m, 8H), 7.24 (q, $J = 7.3$ Hz, 16H), 7.31 (tt, $J_1 = 7.6$ Hz, $J_2 = 1.4$ Hz, 4H), 7.39 (tq, $J_1 = 7.4$ Hz, $J_2 = 1.5$ Hz, 8H), 7.54 (dd, $J_1 = 8.2$ Hz, $J_2 = 1.4$ Hz, 8H), 7.70 (dd, $J_1 = 8.2$ Hz, $J_2 = 1.4$ Hz, 8H) ^{13}C NMR (126 MHz, CDCl_3): δ ppm 127.40, 127.84, 130.17, 130.48, 131.56, 134.03, 134.27, 134.61 ^{29}Si NMR (99 MHz, CDCl_3): δ ppm -79.36 (s, 4Si), -78.10 (s, 4Si), -45.42 (s, 2Si).

3.9 Analytical Techniques

Synthesized materials were evaluated by NMR taking advantage of the three nuclei of the molecules: ^1H , ^{13}C , and ^{29}Si . Crystallized samples (0.05 g) were dissolved in 0.6 ml of CDCl_3 -1%TMS and placed in a Varian UNITY Innova 600 at 500 MHz for ^1H , 126 MHz for ^{13}C , and 99 MHz for ^{29}Si . NMR spectra contain traces of the crystallization solvents including THF, DCM, and Hexanes.

For crystallographic analysis, 0.5 g of each compound was dissolved in THF or DCM and slowly evaporated for 3 days to get crystals. The crystals obtained were mounted on a nylon loop with paratone oil and analyzed on a Bruker APEX-II CCD diffractometer. The crystal was kept at a constant temperature of 173 K during data collection.

Mixtures were prepared by mixing two or three components in solid state and dissolving the mixture in DCM. The solvent was then rapidly removed under dynamic vacuum. For differential scanning calorimetry (DSC) experiments, TA Instruments Q2000 equipped with a mechanical cooler was used. The temperature was equilibrated to 50 °C for 2 min, a constant heating rate of 5 K/min up to a determined temperature above melting. Cooling traces were obtained by cooling from above complete melting at a constant cooling rate of 5 K/min up to 50 °C. A second heating ramp with the same rate as the 1st was used to verify the reproducibility and possible thermal degradation that may occurred during the 1st heating cycle. No thermal degradation was observed.

Thermogravimetric analysis was run in a TGA Q50 apparatus from TA instruments. In this, a platinum pan was loaded with a sample weight of 8 mg \pm 0.2 mg. The experiment was run under dry nitrogen stream at a flow rate of 100 ml/min.

The samples were equilibrated at 323.15 K and heated to 1073.15 K at a rate of 20 K/min.

4 Results and Discussion

4.1 Pure Components

4.1.1 Crystallography

The crystal structure of each compound was obtained by X-ray diffraction from a well-prepared single crystal of each compound. Details on the crystal growth conditions are described in the SI. The unit cell information is depicted in Table 1. There is no apparent specific trend to correlate the packing density with either the size of the R moiety or the overall molecular weight of each compound.

From the analysis of the intramolecular configuration, depending on the R group, there are differences in the distances between the C1 and C2 phenyls and between the C3 and C4 phenyls, as well as differences in the internal angles within the silsesquioxane core as depicted in Scheme 2. These findings suggest that to accommodate the R groups, the phenyl group bonded to the T-silicon (the silsesquioxane deck) needs to be asymmetrically twisted, affecting the overall crystallographic packing density. Interestingly, despite a similar chemical configuration, these structures do not pack in a similar fashion. The distances and angles listed in Table 2 provide an idea of how the selection of R affects the internal structure configuration. The angles Si1-O1-Si0 and Si2-O2-Si0, where Si1 and Si2 are the T-silicon and Si0 is the D-silicon were the same for R = methyl. As the length of the R group increases from methyl to *n*-butyl, an increasing mismatch between these two angles emerge. A similar trend was also observed for cycloaliphatic moieties. It is interesting to point out that the angle of O1-Si0-O2 did not change significantly regardless of the type of R group used, except for R = phenyl.

4.1.2 Phase Behavior

Melting and recrystallization of all 7 pure DDSQ-2R₂ compounds was investigated using a differential scanning calorimetry (DSC) with a heating-cooling-heating cycle. Thermal characteristics of these compounds were analyzed using the cooling and the 2nd heating DSC traces of normalized heat flow versus temperature. The ramp rate for both cooling and heating was at 5 K/min.

DSC traces of cooling and heating for DDSQ-2Me₂ are shown in Fig. 1a. The other six compounds have similar DSC traces. Cooling DSC traces at a rate of 5 K/min resulted in a sharp exotherm for all seven compounds, indicating rapid crystallization growth for all seven compounds. In Fig. 1b, melting traces for all seven compounds are shown. Melting

Table 1 Parameters for pure components from X-ray diffraction analysis

R	MW (g/mol)	Unit cell length (Å)	Unit cell angle (°)	Unit cell volume (Å) ³	Space group	Density (g/cm ³)
methyl	1181.81	a 14.93	α 90	5852.3	P 4 ₂ /m	1.341
		b 14.93	β 90			
		c 26.27	γ 90			
ethyl	1237.94	a 11.06	α 88.77	3050.0	P -1	1.348
		b 12.60	β 81.76			
		c 22.31	γ 82.40			
<i>n</i> -butyl	1350.12	a 13.18	α 88.33	3468.3	P-1	1.293
		b 13.19	β 86.09			
		c 20.00	γ 89.73			
<i>i</i> -propyl	1294.03	a 23.02	α 90	6678.5	C 2/c	1.287
		b 14.02	β 103.12			
		c 21.25	γ 90			
cyclopentyl	1398.16	a 17.18	α 90	7094.1	P bca	1.309
		b 19.52	β 90			
		c 21.14	γ 90			
cyclohexyl	1454.28	a 25.95	α 90	8171.6	C 2/c	1.299
		b 13.83	β 113.49			
		c 24.82	γ 90			
phenyl	1430.08	a 11.11	α 70.12	1735.9	P -1	1.368
		b 12.36	β 76.24			
		c 14.21	γ 73.13			

and recrystallization characteristics including the onset temperature of crystallization from the melt, T_c , the onset melting temperature, T_m , the undercooling for recrystallization, the heat of fusion for melting, ΔH_m , and the change of entropy at melting, ΔS_m , for pure DDSQ-2R₂ are reported in Table 3. It was also noted that the exothermic heat released during the crystallization from the melt and the heat of fusion for melting were identical within the experimental error.

For R = Me, Et, and *n*-Bu, T_m decreases, and ΔH_m also decreases as the number of carbons in R increases. In contrast, for R = CyP, and CyH, increases of T_m and ΔH_m were observed as the number of carbons increases for cycloaliphatic moieties. It was interesting

that when comparing R = Ph with the cycloaliphatic R groups, a lower value of T_m was observed but with a higher value ΔH_m . The higher value of ΔH_m may be associated with the high crystal density observed for DDSQ-2Ph₂, which had one of the highest packing density. The combination of the low value of T_m and the high packing density indicates that the interaction between phenyl rings has lower intermolecular forces as compared with those of fully saturated cyclic moieties. The undercooling was lowest for R = *n*-butyl, only 2 K, while highest for R = Phenyl, around 64 K. This observation suggests as the R group becomes more flexible, the energy barrier for crystallization diminishes.

Table 2 Distances and angles calculated from the modelled crystal structures. Refer to Scheme 2 for atom notations

R	methyl	Ethyl	<i>n</i> -butyl	<i>i</i> -propyl	cyclopentyl	cyclohexyl	phenyl
Distance (Å)							
C1-C2	12.48	13.03	12.76	12.31	12.17	11.99	13.11
C3-C4	7.87	7.59	8.33	7.05	5.67	7.10	6.24
Angle (°)							
Si1-O1-Si0	156.1	154.0	202.8	167.4	157.5	164.8	140.5
Si2-O2-Si0	156.1	148.6	136.6	148.9	146.3	146.9	134.6
O1-Si0-O2	107.6	108.7	106.1	109.9	111.7	108.4	125.0

Table 3 Melting temperature (T_m), crystallization temperature (T_C) at a heating rate and a cooling rate of 5 K/min, undercooling ($\Delta T = T_m - T_C$), change in enthalpy at melting (ΔH_m), and change in entropy at melting (ΔS_m) calculated from $\Delta S_m = \Delta H_m/T$ for individual components

R	T_m (K)	T_C (K)	ΔT (K)	ΔH_m (kJ/mol)	ΔS_m (J/mol·K)
Methyl	546	515	31	53.36	97.76
Ethyl	482	442	40	41.38	85.90
<i>n</i> -butyl	416	414	2	31.62	75.97
<i>i</i> -propyl	565	525	40	42.16	74.66
Cyclopentyl	533	518	15	26.61	49.95
Cyclohexyl	555	512	43	33.39	60.14
Phenyl	526	462	64	48.11	91.42

Finally, the use of *i*-propyl as R produced a DDSQ compound with the highest T_m . Interestingly, the crystal packing density is also the lowest for DDSQ-2*i*Pr₂.

The change of entropy at melting, ΔS_m , is an indicator for the feasibility to disrupt the intermolecular packing. All calculated ΔS_m can be seen in Table 3. Reduction of ΔS_m was observed when the molecular weight and the density of packing increased when R was linear. From the structures functionalized with R = CyP, CyH, and Ph, it was found that the highest ΔS_m was attributed to DDSQ-2Ph₂, and the lowest was attributed to R = CyP. It is to highlight that DDSQ-2Ph₂ is also the structure with the highest calculated density, as shown in Table 1. This observation indicates that there may be weak intermolecular Van der Waals type of interactions between phenyl rings. It was then decided to relate the unit cell parameters with T_m . From this analysis, it was deduced that T_m is dependent on the type of unit cell, with a P -1 cell exhibiting the lowest melting temperatures followed by P 4₂/m and P bca, which possess similar angles. The type of unit cell with the highest melting temperatures was observed for C

2/c. Work to further understand how the R group influenced the packing structure is currently ongoing.

Based on DSC results, a sublimation chamber containing DDSQ-2Ph₂ powder was placed in a 270 °C oil bath while under vacuum. A white solid layer was formed on the surface of the cold finger inside the sublimator. The formed layer was collected and analyzed by ¹H, ¹³C, and ²⁹Si NMR. Spectra after sublimation were identical to those of the starting DDSQ-2Ph₂ (see supplementary information (SI)). Therefore, DDSQ-2Ph₂ can exist in the vapor phase without decomposition. This finding is a unique behavior not observed in fully condensed octaphenyl and dodecaphenyl polyhedral oligomeric silsesquioxanes [28, 29]. This finding means that the presence of siloxanes in the DDSQ core provides flexibility to the structure. The experiment was repeated with DDSQ-2Me₂, achieving similar results. The samples were then analyzed by TGA to verify vaporization behavior, as shown in Fig. 2. An equimolar mixture of DDSQ-2Ph₂ and DDSQ-2Me₂ was prepared by the dissolution of both components in dichloromethane (DCM) followed by solvent evaporation. The mixture was then analyzed by TGA. Interestingly, the 5% loss temperature was lower than that of the pure components. This observation suggests the miscibility of these two compounds at the molten-state. The 5% and 50% weight loss temperature for each sample are summarized in Table 4. These results are evidence of the existence of an azeotropic mixture between DDSQ-2Me₂ with DDSQ-2Ph₂.

4.2 Binary Mixtures

Based on the existence of an azeotrope between two different DDSQ-2R₂ and different crystallographic structures, we proposed that these binary mixtures might also form ideal eutectic. Supported by prior literature on DDSQ-2(RR') mixtures, it was assumed that the binary systems composed DDSQ-2R₂

Fig. 1 DSC results for individual DDSQ-2R₂. Second heating and first cooling for DDSQ-2Me₂ (a), and second heating for all samples evaluated in this work (b)

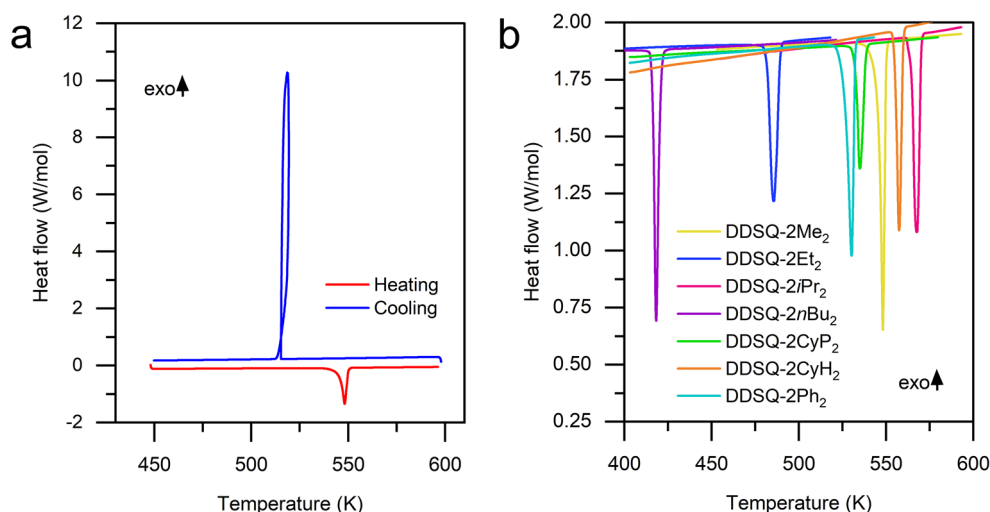


Table 4 The 5% and 50% weight loss temperature evaluated by TGA for pure DDSQ-2Me₂, pure DDSQ-2Ph₂, and a 1:1 mixture between both components

Weight loss	DDSQ-2Me ₂	DDSQ-2Ph ₂	DDSQ-2Me ₂ /DDSQ-2Ph ₂ 1:1 mixture
5%	662 K	697 K	635 K
50%	727 K	764 K	728 K

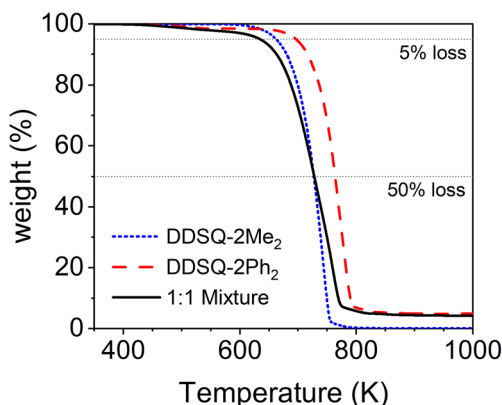
are not miscible in the solid-state [19]. The eutectic temperatures (T_E) and the eutectic compositions (x_E) for binary mixtures were calculated using the Gibbs free melting energy approach assuming ideal behavior or activity coefficient equal to one

$$G = RT \ln(x_i) + \Delta H_{mi} \frac{T_{mi} - T}{T_{mi}} \quad (1)$$

$$\sum_{i=1}^{i=n} x_i = 1 \quad (2)$$

The set of eqs. 1 and 2 was solved by an iterative method in which the total free energy (G) was minimized with the assumed ideal behavior. The subscript i represents each component in the mixture. Binary mixtures were prepared based on the calculated compositions. The mixtures were dissolved in DCM and fast dried under dynamic vacuum. The resultant homogeneous mixtures were then analyzed by DSC. Table 5 compiles the calculated and experimental eutectic compositions and temperatures. Traces of the second heating and cooling for each binary mixture can be seen in the SI. For most of the binary mixtures investigated, a sharp cooling exothermic peak was observed, as also seen in the SI.

DSC traces for the prepared binary mixtures have a sharp endothermic peak below the T_m of the two pure components in the mixture. This sharp transition temperature was identified as the eutectic temperature, T_E . This depression in T_m indicates that the binary mixtures have a eutectic temperature. It was decided to compare the change in the enthalpy at T_m for mixtures ($\Delta H_{m(\text{mixture})}$) obtained experimentally against a calculated $\Delta H_{m(\text{mixture})}$ obtained from Eq. 3. This calculation again assumes ideal eutectic behavior.

**Fig. 2** TGA results for individual DDSQ-2R₂

$$\Delta H_{m(\text{mixture})} = \sum_{i=1}^n x_i \Delta H_{mi} \quad (3)$$

Similar values between the calculated and experimental $\Delta H_{m(\text{mixture})}$ observed in Table 5 represents ideal systems, or non-miscibility in the solid-state. On the other hand, systems with large differences between the calculated and the experimental $\Delta H_{m(\text{mixture})}$ are believed to have partial miscibility in the solid-state. A comparison between the calculated and the experimental $\Delta H_{m(\text{mixture})}$ as well T_E , indicated that the solid phase of DDSQ-2Me₂ exhibited a partial solubility only with DDSQ-2CyP₂. Interestingly, these two structures have similar space groups, indicates the partial-miscibility in the solid-state requires similar crystallographic structures, which is consistent with the mixing of elemental solids. DDSQ-2iPr₂ and DDSQ-2CyH₂ have the same space group; when mixed, the experimental $\Delta H_{m(\text{mixture})}$ decreased in comparison with the calculated value.

In contrast, most of the mixtures containing structures that pack in the space group P-1 have partial miscibility in the solid-state, this observation indicates the structures with a P-1 space group can be more easily interrupted by other compounds in the mixture, therefore reducing the enthalpy at melting. Another interesting finding was observed for the DDSQ-2CyP₂ and DDSQ-2CyH₂ mixture. A sharp melting peak in the DSC trace was located between the melting peaks of the pure materials. This suggests full-miscibility between DDSQ-2CyP₂ and DDSQ-2CyH₂ in the solid-state. In addition, the difference between calculated and experimental $\Delta H_{m(\text{mixture})}$ is also very small. However, these two compounds have different crystallographic space group. Hence, it is hypothesized that the structural similarity between these molecules allows crystallization in a single structure shared for both materials; this behavior suggests that intermolecular forces can affect the intramolecular configuration of the DDSQ core.

4.3 Ternary Mixtures

Two ternary systems were selected and mixed based on the results of binary mixtures with clear eutectic compositions. The first chosen ternary system was composed by DDSQ-2Me₂, DDSQ-2CyP₂, and DDSQ-2Ph₂, which we term system-1. This was selected as all three binary mixtures have very clear eutectic transition as shown by DSC measurement (see SI) and the eutectic compositions are between 40 mol% to

Table 5 Calculated and experimentally mixed binary eutectic molar compositions¹

Compound A		DDSQ-2Ph ₂			DDSQ-2CyH ₂			DDSQ-2CyP ₂			DDSQ-2 <i>i</i> Pr ₂			DDSQ-2 <i>n</i> Bu ₂			DDSQ-2Et ₂		
		x _E	T _E K	ΔH _m kJ/ mol	x _E	T _E K	ΔH _m kJ/ mol	x _E	T _E K	ΔH _m kJ/ mol	x _E	T _E K	ΔH _m kJ/ mol	x _E	T _E K	ΔH _m kJ/ mol	x _E	T _E K	ΔH _m kJ/ mol
DDSQ-2Me ₂	Calculated	0.38	505	52	0.46	512	44	0.33	500	37	0.54	519	49	0.02	415	32	0.16	474	44
	Experimental	0.43	510	48	0.51	514	44	0.37	494	27	0.56	524	46	0.02	405	28	0.17	478	39
DDSQ-2Et ₂	Calculated	0.75	469	44	0.74	469	44	0.62	461	37	0.83	473	42	0.15	409	33			
	Experimental	0.78	428	15	0.77	426	14	0.65	447	15	0.84	488	41	0.16	395	21			
DDSQ-2 <i>n</i> Bu ₂	Calculated	0.95	414	32	0.92	412	32	0.84	409	31	0.04	414	32						
	Experimental	0.95	410	28	0.92	418	26	0.84	420	22	0.04	412	27						
DDSQ-2 <i>i</i> Pr ₂	Calculated	0.36	507	47	0.43	516	38	0.32	501	32									
	Experimental	0.38	*		0.46	497 [†]	9	0.34	507 [†]	20									
DDSQ-2CyP ₂	Calculated	0.58	489	36	0.60	492	30												
	Experimental	0.59	497	18	0.61	538 [♠]	32												
DDSQ-2CyH ₂	Calculated	0.45	500	43															
	Experimental	0.45	510	17															

Calculated and experimental eutectic temperature T_E, and ideal change of enthalpy at melting ΔH_m. Ideal calculations were made by minimization of Gibbs free energy. Experimental results for x_E are reported after weight the sample in the laboratory and back-calculation of the moles in the sample, experimental eutectic temperature was obtained from the onset in the first peak, and experimental ΔH_m calculated from the first peak area after DSC. x_E is given for compound A in each mixture. Notes: * Endotherm below melting temperature of pure compounds reported in Table 3 was not observed. † Broad melting transitions below the T_m of the pure components reported in Table 3. ♠ melting temperature between the T_m of the pure components reported in Table 3

60 mol%, which allows for more accurate preparation for the ternary eutectic mixture. The second system was DDSQ-2Me₂, DDSQ-2Et₂, and DDSQ-2*i*Pr₂, termed system-2. Similar to system-1, all three binary mixtures of system 2, when mixed at the eutectic composition, exhibited a sharp eutectic transition in heating and a sharp solidification in cooling. Also, the eutectic point in these three binary eutectics matches well with the ideal eutectic prediction (Table 5). Due to the lower value of T_m for DDSQ-2Et₂ some care was needed in preparing the ternary eutectic sample. The ternary eutectic composition for both systems was first determined graphically, as seen in Fig. 3a and Fig. 3c.

The ternary eutectic point (composition, C_{TE}, and temperature, T_{TE}) for system-1 and system-2 was calculated based on Eq. 1 and Eq. 2 with an iterative approach similar to the calculation performed for the binary mixtures. For simplicity, ideal eutectic was assumed. As expected, the calculated value of C_{TE} is the same as the graphically determined C_{TE}. Mixtures were prepared in the laboratory using the calculated ternary eutectic compositions, then solubilized in DCM and fast dried under dynamic vacuum. The thermal characteristics of system-1 and system-2 were again evaluated using DSC similar to the binary case. Results are shown in Fig. 3b and d, respectively. It was observed that system-1 has a melting endotherm peak at about 488 K as observed in Fig. 3b. This value was about

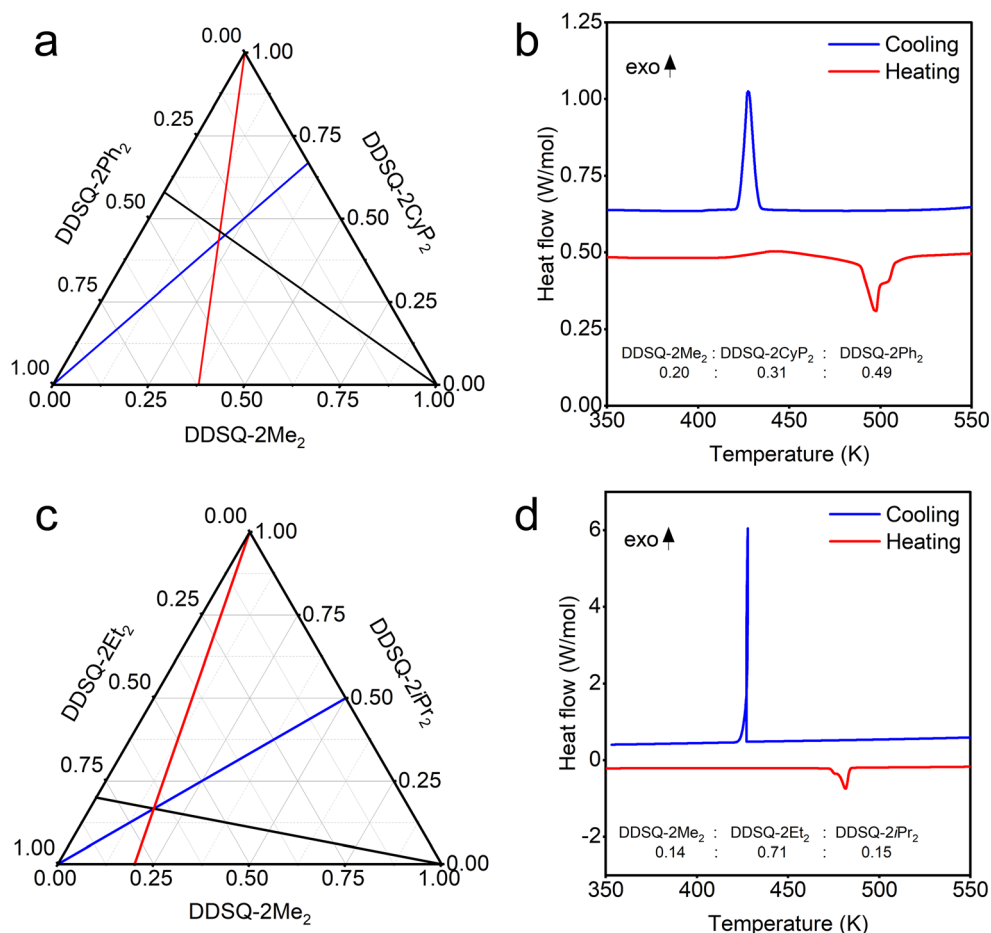
10 K higher than the predicted value of 478 K based on the ideal eutectic assumption. This value was also lower than the other three binary eutectic temperatures as well as the melting temperature of three pure components. It was worthwhile to mention here that the observed endotherm peak was broader than predicted. This draws into question the assumption of ideality, hence the composition used was not exactly the ternary eutectic composition.

Figure 3d show the DSC traces of system-2 composed of DDSQ-2Me₂, DDSQ-2Et₂, and DDSQ-2*i*Pr₂. A sharp melting endotherm peak for system-2 was observed at 473 K, which was about 10 K lower than the melting temperature of DDSQ-2Et₂ and 5 K lower than the observed binary eutectic temperature of DDSQ-2Me₂/DDSQ-2Et₂. The predicted value of T_{TE} based on ideal eutectic assumption was 467 K. Additionally, as shown in Fig. 3d, upon cooling, a sharp exotherm solidification peak was observed. This observation suggests the composition used for system-2 should be very close to the true ternary eutectic point.

5 Conclusion

The interaction between the organic moiety bonded to the D-Si and the phenyl-group bonded to the T-Si of

Fig. 3 Ternary phase diagram calculated from binary eutectic compositions (a) and DSC traces of first cooling and second heating for DDSQ-2Me₂:DDSQ-2CyP₂:DDSQ-2Ph₂ (0.20:0.31:0.49) (b). Ternary phase diagram calculated from binary eutectic compositions (c) and DSC traces of first cooling and second heating for DDSQ-2Me₂:DDSQ-2Et₂:DDSQ-2iPr₂ (0.14:0.71:0.15) (d)



the adjacent DDSQ molecules plays a pronounced effect over the structure by changing the internal configuration of DDSQ cage. Thermal analysis of individual structures shows that for DDSQ compounds with linear aliphatic moieties attached to the D-Si, as the number of carbon increases from methyl to *n*-butyl, the value of T_m dropped from 546 K to 416 K. This behavior was opposite when the cycloaliphatic moiety was bonded to the D-Si. As when the moiety changes from cyclopentyl to cyclohexyl, the value of T_m increases from 533 K to 555 K. It was interesting and also surprising to find DDSQ-2*i*Pr₂ has the highest melting temperature while the crystalline density was the lowest. Despite the chemical similarity between methyl, ethyl, and *n*-butyl, binary mixtures of these fully-condensed DDSQ compounds exhibit eutectic characteristics in which mixtures are miscible in the liquid and gas phases and immiscible in the solid phase. Furthermore, it was possible to form a ternary eutectic. However, DDSQ-2CyP₂ and DDSQ-2CyH₂ exhibit isomorphic mixing. These results suggest the internal configuration and the flexibility of organic moiety bonded to the D-Si can result in solid-state

segregation. This finding may result in the self-assembly of DDSQ structures when solidify from a liquid mixture. Further investigations are needed to fully explore the potential applications of DDSQ compounds.

Supplementary Information The online version contains supplementary material available at <https://doi.org/10.1007/s12633-021-01470-0>.

Acknowledgments Authors are grateful to Drs. Daniel Holmes, Richard Staples and Ms. Emily Dong for their support of NMR, X-ray crystallography and DSC studies, respectively. Additionally, Dr. Jairo Perilla from Universidad Nacional of Colombia for his collaboration and valuable discussion.

Code Availability Not applicable.

Authors' Contributions Not applicable.

Funding This work was partially supported by the Office of Naval Research (N00014-16-2109) for generous funding.

Data Availability Materials and equipment used for this work are described within the manuscript. In addition, experimental details, spectral information, crystal structures, DSC traces, and phase diagrams are also provided in **supplementary information**.

Declarations

Conflicts of Interest/Competing Interests All authors declare there are no conflicts or competing interests.

Ethics Approval and Consent to Participate The work described is original and has not been published before in any form of language; it is not under consideration for publication elsewhere; all authors had reviewed and approved the manuscript and supplementary information.

Consent to Publication Yes

References

- Schoen BW, Holmes D, Lee A (2013) Identification and quantification of cis and trans isomers in aminophenyl double-decker silsesquioxanes using ¹H-29Si gHMBC NMR. *Magn Reson Chem* 51:490–496. <https://doi.org/10.1002/mrc.3962>
- Schoen BW, Lira CT, Lee A (2014) Separation and solubility of Cis and trans isomers in nanostructured double-Decker Silsequioxanes. *J Chem Eng Data* 59:1483–1493. <https://doi.org/10.1021/jc4010245>
- Seurer B, Vij V, Haddad T, Mabry JM, Lee A (2010) Thermal transitions and reaction kinetics of Polyhedral Silsesquioxane containing Phenylethynylphthalimides. *Macromolecules* 43:9337–9347. <https://doi.org/10.1021/ma101640q>
- Moore LMJ, Zavala JJ, Lamb JT, Reams JT, Yandek GR, Guenther AJ, Haddad TS, Ghiassi KB (2018) Bis-phenylethynyl polyhedral oligomeric silsesquioxanes: new high-temperature, processable thermosetting materials. *RSC Adv* 8:27400–27405. <https://doi.org/10.1039/C8RA05954C>
- Hoque MA, Kakihana Y, Shinke S, Kawakami Y (2009) Polysiloxanes with periodically distributed isomeric double-Decker Silsesquioxane in the Main chain. *Macromolecules* 42:3309–3315. <https://doi.org/10.1021/ma900124x>
- Wei K, Wang L, Zheng S (2013) Organic–inorganic polyurethanes with 3,13-dihydroxypropyloctaphenyl double-decker silsesquioxane chain extender. *Polym Chem* 4:1491–1501. <https://doi.org/10.1039/C2PY20930F>
- Tanaka T, Hasegawa Y, Kawamori T, Kunthom R, Takeda N, Unno M (2019) Synthesis of double-Decker Silsesquioxanes from substituted Difluorosilane. *Organometallics* 38:743–747. <https://doi.org/10.1021/acs.organomet.8b00896>
- Mitula K, Dudzic B, Marciniak B (2018) Synthesis of Dialkenyl-substituted double-Decker Silsesquioxanes as precursors for linear Copolymeric systems. *J Inorg Organomet Polym Mater* 28:500–507. <https://doi.org/10.1007/s10904-017-0746-y>
- Walczak M, Januszewski R, Majchrzak M, Kubicki M, Dudzic B, Marciniak B (2017) Unusual cis and trans architecture of dihydrofunctional double-decker shaped silsesquioxane and synthesis of its ethyl bridged π -conjugated arene derivatives. *New J Chem* 41:3290–3296. <https://doi.org/10.1039/C7NJ00255F>
- Żak P, Dudzic B, Dutkiewicz M, Ludwiczak M, Marciniak B, Nowicki M (2016) A new class of stereoregular vinylene-arylene copolymers with double-decker silsesquioxane in the main chain. *J Polym Sci Part A: Polym Chem* 54:1044–1055. <https://doi.org/10.1002/pola.27957>
- Wang M, Chi H, KS J, Wang F (2019) Progress in the synthesis of Bifunctionalized polyhedral oligomeric Silsesquioxane. *Polymers* 11:2098. <https://doi.org/10.3390/polym11122098>
- Beata D, Bogdan M (2017) Double-decker silsesquioxanes: current chemistry and applications. *Curr Org Chem* 21:2794–2813
- Cao J, Fan H, Li B-G, Zhu S (2017) Synthesis and evaluation of double-Decker Silsesquioxanes as modifying agent for epoxy resin. *Polymer* 124:157–167. <https://doi.org/10.1016/j.polymer.2017.07.056>
- Xu S, Zhao B, Wei K, Zheng S (2018) Organic-inorganic polyurethanes with double decker silsesquioxanes in the main chains: morphologies, surface hydrophobicity, and shape memory properties. *J Polym Sci B Polym Phys* 56:893–906. <https://doi.org/10.1002/polb.24603>
- Liu N, Wei K, Wang L, Zheng S (2016) Organic–inorganic polyimides with double decker silsesquioxane in the main chains. *Polym Chem* 7:1158–1167. <https://doi.org/10.1039/c5py01827g>
- Liu N, Li L, Wang L, Zheng S (2017) Organic-inorganic polybenzoxazine copolymers with double decker silsesquioxanes in the main chains: synthesis and thermally activated ring-opening polymerization behavior. *Polymer* 109:254–265. <https://doi.org/10.1016/j.polymer.2016.12.049>
- Wu S, Hayakawa T, Kakimoto M-A, Oikawa H (2008) Synthesis and characterization of Organosoluble aromatic polyimides containing POSS in Main chain derived from double-Decker-shaped Silsesquioxane. *Macromolecules* 41:3481–3487. <https://doi.org/10.1021/ma7027227>
- Jiang Q, Zhang W, Hao J, Wei Y, Mu J, Jiang Z (2015) A unique “cage–cage” shaped hydrophobic fluoropolymer film derived from a novel double-decker structural POSS with a low dielectric constant. *J Mater Chem* 3:11729–11734. <https://doi.org/10.1039/C5TC02432C>
- Wang Z, Yonggang L, Huijuan M, Wenpeng S, Tao L, Cui fen L, Junqi N, Guichun Y, Zuxing C (2018) Novel phosphorus-nitrogen-silicon copolymers with double-decker silsesquioxane in the main chain and their flame retardancy application in PC/ABS. *Fire Mater* 2:16230–16957. <https://doi.org/10.1002/fam.2649>
- Vogelsang DF, Maleczka RE, Lee A (2019) Predictive liquid chromatography separation for mixtures of functionalized double-Decker shaped Silsesquioxanes based on HPLC chromatograms. *Ind Eng Chem Res* 58:403–410. <https://doi.org/10.1021/acs.iecr.8b05490>
- Vogelsang DF, Dannatt JE, Schoen BW (2019) Phase behavior of cis-trans mixtures of double-decker shaped Silsesquioxanes for Processability enhancement. *ACS App Nano* 2:1223–1231. <https://doi.org/10.1021/acsanm.8b02114>
- Vogelsang DF, Maleczka RE, Lee A (2019) HPLC characterization of cis and trans mixtures of double-Decker shaped Silsesquioxanes. *Silicon Chem* 11:5–13. <https://doi.org/10.1007/s12633-018-0045-4>
- Clavaguera N, Saurina J, Lheritier J, Masse J, Chauvet A, Clavaguera-Mora MT (1997) Eutectic mixtures for pharmaceutical applications: a thermodynamic and kinetic study. *Thermochim Acta* 290:173–180. [https://doi.org/10.1016/S0040-6031\(96\)03077-8](https://doi.org/10.1016/S0040-6031(96)03077-8)
- Fiala S, Brown MB, Jones SA (2011) Dynamic in-situ eutectic formation for topical drug delivery. *J Pharm Pharmacol* 63:1428–1436
- Lee A, Lu Y, Roche A, Pan T-Y (2016) Influence of Nanostructured Silanols on the microstructure and mechanical properties of A407 and A359 aluminum casting alloys. *Int J Met* 10:338–341. <https://doi.org/10.1007/s40962-016-0044-4>
- Liu S, Ma L, Shu Y, Subramanian KN, Lee A, Guo F (2014) Effects of POSS-Silanol addition on whisker formation in Sn-based Pb-free electronic solders. *J Electron Mater* 43:26–32. <https://doi.org/10.1007/s11664-013-2672-2>
- Brostow W, Goodman SH, Wahmund J (2013) In: Dodiuk H and Goodman SH (ed) *Handbook of Thermoset Plastics*, 3rd edn. Elsevier, Oxford, UK
- Fina A, Tabuani D, Camiato F, Frache A, Boccaleri E, Camino G (2006) Polyhedral oligomeric silsesquioxanes (POSS) thermal

degradation. *Thermochim Acta* 440:36–42. <https://doi.org/10.1016/j.tca.2005.10.006>

29. Blanco I, Abate L, Bottino FA (2017) Mono substituted octaphenyl POSSs: the effects of substituents on thermal properties and solubility. *Thermochim Acta* 655:117–123. <https://doi.org/10.1016/j.tca.2017.06.019>

Publisher's Note Springer Nature remains neutral with regard to jurisdictional claims in published maps and institutional affiliations.